November, 1981] © *1981 The Chemical Society of Japan* *Bull. Chem. Soc. Jpn.*, **54**, *3361—3365 (1981)* 3361

Kinetics of Monomerization or Polymerization Reaction for Bis(*N*-phenylsalicylideneaminato)nickel(II) and Bis(*N*-methylsalicylideneaminato)nickel(II) in Solid Phase

Kikuo Miyokawa,* Hidenori Hirashima, and Isao Masuda
Department of Chemistry, Faculty of Science, Fukuoka University, Nanakuma, Nishi-ku, Fukuoka 814-01

(Received January 12, 1981)

A kinetic investigation was carried out by means of a thermomagnetic analysis on two structural transformation reactions in solid phase: monomeric square planar-to-polymeric octahedral for Ni(*N*-Me-salam)$_2$ and polymeric octahedral-to-monomeric square planar for Ni(*N*-Ph-salam)$_2$. The polymerization process followed the Avrami-Erofeev equation ($n=2$) with $E_a=303$ kJ/mol and the monomerization followed the first order equation with $E_a=78$ kJ/mol. The thermal pyridine liberating reaction of Ni(*N*-Ph-salam)$_2$py$_2$, involving an octahedral-to-square planar transformation, has been investigated isothermally and found to follow the first order equation with $E_a=167$ kJ/mol.

Extensive investigations of the nickel(II) complexes having the formula Ni(*N*-R-X-salam)$_2$ (where *N*-R-X-salam represents an anion of the Schiff bases derived from the ring-substituted salicylaldehydes X-sal and amine R–NH$_2$) have revealed that the complexes exist in several structural forms with different coordination geometries: *i.e.*, square planar,[1)] tetrahedral,[1–3)] dimeric square bi-pyramidal,[4)] and polymeric octahedral[5,6)] structures. Isomerization reactions in solid phase have also been found to occur for some complexes of these structural forms.[3,6–9)] However, the kinetics of the isomerization reaction has remained ambiguous.

In this work, the kinetics of the transformation reactions in solid phase, monomer-to-polymer of Ni(*N*-Me-salam)$_2$ and polymer-to-monomer of Ni(*N*-Ph-salam)$_2$, have been investigated by means of a thermomagnetic analysis measuring magnetic susceptibility changes of the sample under isothermal or dynamic conditions.

Experimental

Materials. Diamagnetic dark green complexes, Ni(*N*-Me-salam)$_2$ and Ni(*N*-Ph-salam)$_2$ (Form I), were prepared by the published procedure.[7,8,10,11)] The paramagnetic light green modification (Form II) of Ni(*N*-Ph-salam)$_2$ was prepared in the following manner: the Form I complex was saturated into dichloromethane (50 ml) at *ca.* 35 °C, then to the solution was added ethanol (50 ml). The mixture was kept at room temperature under stirring until light green crystals separated.

The bis(pyridine) adduct Ni(*N*-Ph-salam)$_2$py$_2$ was precipitated from pyridine solution saturated with the Form I complex by addition of ethanol.

Found for Form II: C, 69.07; H, 4.51; N, 6.39; Ni, 13.19%. Calcd for $C_{26}H_{20}N_2O_2Ni$: C, 69.22; H, 4.44; N, 6.21; Ni, 13.02%. Found for the pyridine adduct: Ni, 9.75%. Calcd for $C_{36}H_{30}N_4O_2Ni$: Ni, 9.64%.

Neodymium oxide was purified by repeating the following procedure: commercial reagent grade Nd_2O_3 was dissolved in aqueous HCl, and the solution was evaporated to dryness. The residue was dissolved in water, and to the resulting solution was added aqueous oxalic acid to precipitate neodymium oxalate. The oxalate thus obtained was collected on a filter, and then pyrolyzed at *ca.* 800 °C to give Nd_2O_3. The purity was ascertained by Nd-content analysis using the EDTA titration method.

Measurements. Thermogravimetric (TG) and differential scanning calorimetric (DSC) curves, and X-ray powder diffraction patterns were recorded as described in a previous paper.[12)] Reflectance spectra were measured by means of an opal glass method[13)] using a Shimadzu MPS 5000 spectrophotometer. The isothermal weight-loss measurements were made with a Sinku Riko micro DTA apparatus TGD-3000-RH, under a constant flow of nitrogen.

A thermomagnetic analysis[14)] was carried out by using a thermomagnetic analysis instrument which was constructed by assembling a Faraday type magnetobalance and an infrared lamp furnace.[15)] The sample was heated at a constant heating rate or kept at a desired temperature with a Sinku Riko temperature controller HPC-3000. On this instrument the following thermomagnetic curves were recorded: the isothermal thermomagnetic curve (hereafter abbreviated as ITM curve), obtained by plotting the magnetic susceptibility change of the sample against time while it was kept under isothermal conditions; the sample was usually heated to the desired temperature at a heating rate of 200 °C min^{-1}; and the dynamic thermomagnetic curve (DTM curve), obtained by plotting the magnetic susceptibility change of the sample under dynamic conditions against temperature; the sample was usually heated at a heating rate 1 °C min^{-1}. These measurements were carried out in a nitrogen atmosphere. The magnetobalance was calibrated by using $[Ni(en)_3]S_2O_3$ and Nd_2O_3, and the strenght of the applied magnetic field was regulated to an appropriate constant value around 0.85 T.

Results

The magnetic and electronic spectral data of the complexes in the solid state are given in Table 1. Whereas the dark green Form I isomer of Ni(*N*-Ph-salam)$_2$ is diamagnetic and is considered to have a square planar structure,[10)] the light green Form II

Table 1. Magnetic and electronic spectral data

Complex	μ_{eff}[a)]	ν_{max}[b)]
	μ_B	10^3 cm^{-1}
Ni(*N*-Ph-salam)$_2$, Form I	dia[c)]	16.3
Ni(*N*-Ph-salam)$_2$, Form II	3.28	10.1, 16.6
Ni(*N*-Ph-salam)$_2$py$_2$	3.09	9.9, 16.8
Ni(*N*-Me-salam)$_2$	dia	16.6
Ni(*N*-Me-salam)$_2$	3.30[d)]	12.7, 18.0

a) Determined at room temperature, 22—25 °C. b) Powder reflectance. c) dia: Diamagnetic. d) See Refs. 7 and 8.

isomer prepared in the present work is paramagnetic with $\mu_{\mathrm{eff}}=3.28\,\mu_{\mathrm{B}}$. The electronic reflectance spectrum of the Form I isomer exhibits a peak with the maximum at $16.3\times10^3\,\mathrm{cm}^{-1}$ ascribed to the square-planar crystal field band of Ni(II), ${}^1A_{1g}\rightarrow{}^1A_{2g}$ transition,[16] while the spectrum of the Form II isomer is composed of two peaks with the maxima at 10.1 and $16.6\times10^3\,\mathrm{cm}^{-1}$; these may be ascribed respectively to the ${}^3A_{2g}\rightarrow{}^3T_{2g}$ and ${}^3A_{2g}\rightarrow{}^3T_{1g}(F)$ transitions of the octahedral crystal field bands.[16] The paramagnetism and the spectral data are indicative of an octahedral coordination and hence a polymeric structure for the Form II isomer.

The TG and DSC curves of the Form I and II isomers of Ni(*N*-Ph-salam)$_2$ are shown in Figs. 1-a and -b. No weight-loss is observed up to 320 °C in these TG curves. In the DSC curves of both isomers, however, an endothermic peak is observed at 280 °C due to the melting. An exothermic peak at 210 °C observed for the Form II isomer may be attributed to the transformation reaction into the Form I isomer. The X-ray diffraction pattern of the product obtained by heating the Form II isomer at 230 °C coincided with that of the Form I isomer.

As for diamagnetic Ni(*N*-Me-salam)$_2$, the TG curve shown in Fig. 1-c exhibits no weight-loss up to 290 °C; the DSC curve shows two endothermic peaks due to the melting at 215 and 302 °C. The former melting is found to be followed by the solidification of the melt; this does not disagree with the observation under microscope by Sacconi *et al.*[7] On heating diamagnetic Ni(*N*-Me-salam)$_2$ at 230 °C, a paramagnetic complex was obtained which showed quite different X-ray powder pattern from that of starting diamagnetic complex. Thus, the melting at 215 °C is thought to occur together with the transformation reaction of diamagnetic Ni(*N*-Me-salam)$_2$ into the paramagnetic complex; the latter melts at 302 °C with a partial decomposition.

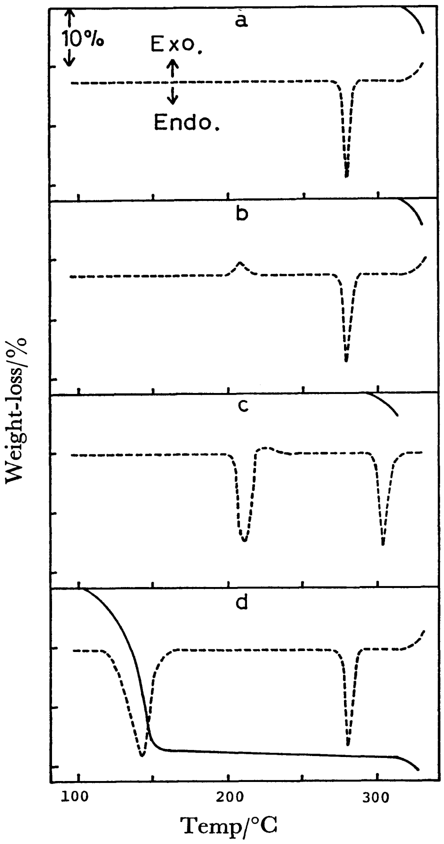

Fig. 1. TG(——) and DSC(- - -) curves; heating rate, 10 °C min^{-1}, in a static air atmosphere.
(a): Ni(*N*-Ph-salam)$_2$ (Form I), (b): Ni(*N*-Ph-salam)$_2$ (Form II), (c): diamagnetic Ni(*N*-Me-salam)$_2$, (d): Ni(*N*-Ph-salam)$_2$py$_2$.

The DTM curve of the paramagnetic Form II isomer of Ni(*N*-Ph-salam)$_2$ is presented in Fig. 2. When *W* mg of the sample is placed in the magnetic field, the response of the electrobalance, *W'* mg, is expressed by Eq. 1:

$$W' = W + W\cdot\chi_g^g\cdot H_c, \tag{1}$$

where χ_g^g is the apparent gram magnetic susceptibility of the sample, and H_c a constant value which is determined by the apparatus and the strength of the applied magnetic field. The DTM curve shown by Fig. 2-a is obtained by plotting $(W'-W)/W$ value *vs.* temperature under dynamic conditions of a heating rate of 1 °C min^{-1}. In this curve a large decrease in the magnetic susceptibility of the Form II isomer is seen in the 170—230 °C region. This may correspond to the transformation reaction of the paramagnetic Form II to the diamagnetic Form I isomer, which is consistent with the results of the thermal analyses. On the basis of the DTM data, $\chi_{\mathrm{Ni(II)}}$, the apparent susceptibility per mole of Ni(II), not corrected for the diamagnetism of all atoms, was calculated by Eq. 2:

$$\chi_{\mathrm{Ni(II)}} = (W'-W)M/(H_cW), \tag{2}$$

where *M* is relative molecular mass of the complex, 450.7. The H_c value has been determined by using

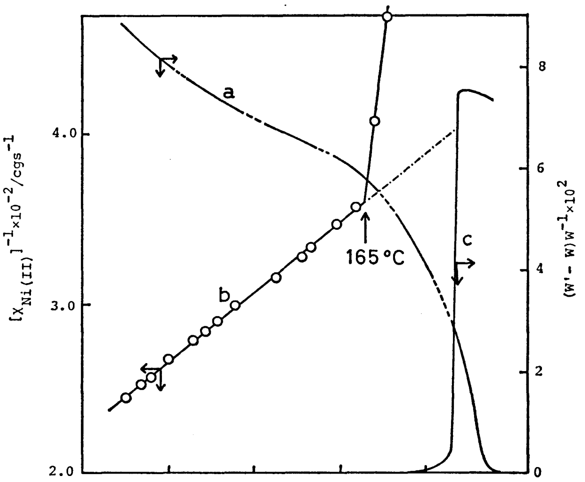

Fig. 2. DTM curve for Ni(*N*-Ph-salam)$_2$ (Form II), (a); plots of reciprocal $\chi_{\mathrm{Ni(II)}}$ *vs.* temperature, for Form II, (b); sample, 18.40 mg. DTM curve for diamagnetic Ni(*N*-Me-salam)$_2$, (c); sample, 18.40 mg. Heating rate, 1 °C min^{-1}. On the dashed line in the curve (a) magnetic-field strength was attenuated to zero to check the base line.

Nd_2O_3 as a standard[17] to be 8.40×10^3 under the present experimental conditions; it is practically constant in the range 25—300 °C. And the plots of reciprocal $\chi_{Ni(II)}$ against temperature give a curve shown by Fig. 2-b. The curve indicates that a Curie-Weiss dependence of the magnetic susceptibility of the Form II isomer is broken at 165 °C; at this temperature the transformation reaction from the Form II to Form I isomer is thought to occur.

The ITM curves for the Form II isomer recorded under isothermal conditions at 175.6, 180.9, 186.1, and 191.3 °C are shown in Fig. 3. The apparent gram susceptibility of the sample, χ_g^s, can be expressed by Eq. 3, where χ_g^{I}, χ_g^{II}, and α are the gram susceptibilities of the Form I and II isomers, and the molar fraction of Form II transformed into Form I, respectively:

$$M \cdot \chi_g^s = [\chi_g^{II}(1-\alpha) + \chi_g^{I} \cdot \alpha]M. \tag{3}$$

Then, the α value is given as

$$\alpha = (\chi_g^s - \chi_g^{II})/(\chi_g^{I} - \chi_g^{II}). \tag{4}$$

The χ_g^{I} value was found to be practically zero and χ_g^{II} was evaluated from a Curie-Weiss dependence, *i.e.*, by extrapolating the linear part below 165 °C of the line in Fig. 2-b to each desired temperature. As shown in Fig. 4, the transformation reaction pursued at four different temperatures is found to be well described by the first order equation: $-\ln(1-\alpha) = kt$, where k and t are the rate constant and time. On the basis of these data, the activation energy E_a and pre-exponential factor A in the Arrhenius equation were determined to be 78 kJ/mol and 1×10^7.

In the case of diamagnetic Ni(*N*-Me-salam)$_2$, the DTM curve shown in Fig. 2-c indicates that the magnetic susceptibility begins to increase gradually at 190 °C, and rapidly increases at ⩾215 °C, which corresponds to the DSC peak temperature due to the melting. The ITM curves recorded at 186.7, 191.3, and 197.7 °C for the transformation to the paramagnetic form are shown in Fig. 5. In this case the χ_g^{I} and χ_g^{II} in Eq. 3 are the gram magnetic susceptibilities of the paramagnetic and diamagnetic Ni(*N*-Me-salam)$_2$, respectively. The χ_g^{I} values at these temperatures were determined after the reaction was completed, and χ_g^{II} was found to be practically zero. As shown

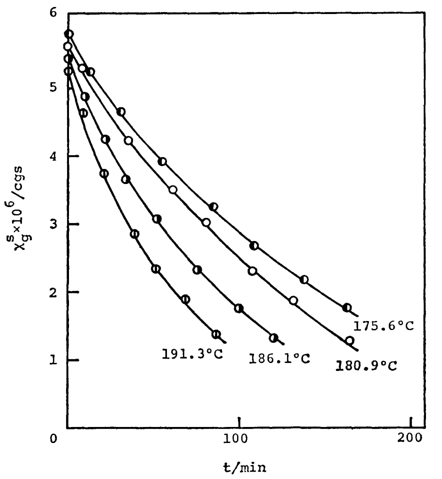

Fig. 3. ITM curves for Ni(*N*-Ph-salam)$_2$ (Form II); polymer-to-monomer transformation under isothermal conditions.

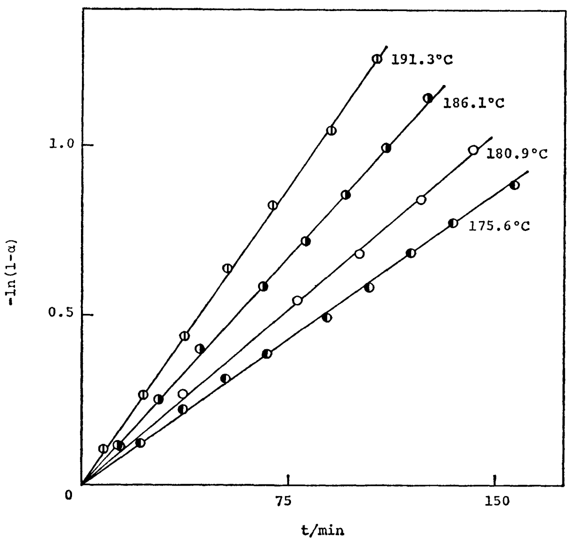

Fig. 4. First order rate plots for polymer-to-monomer transformation of Ni(*N*-Ph-salam)$_2$ (Form II).

TABLE 2. KINETIC DATA OF TRANSFORMATION REACTIONS IN SOLID PHASE

Complex	Reaction Mode	Reaction Scheme	E_a / kJ mol^{-1}	log (A/min^{-1})	k / 10^{-2} min^{-1}	Temp / °C
Ni(*N*-Ph-salam)$_2$	a)	$-\ln(1-\alpha) = kt$	78± 5	7.0±0.6	0.723	175.6
					0.867	180.9
					1.13	186.1
					1.46	191.3
Ni(*N*-Me-salam)$_2$	b)	$-\ln(1-\alpha) = (kt)^2$	303±11	33±2	3.76	186.7
					7.81	191.3
					24.9	197.7
Ni(*N*-Ph-salam)$_2$py$_2$	c)	$-\ln(1-\alpha) = kt$	167±12	22±1	0.668	86.8
					0.937	88.8
					1.23	90.6
					1.73	93.0

a) Polymer-to-monomer. b) Monomer-to-polymer. c) Monomer(octahedral)-to-monomer(square-planar).

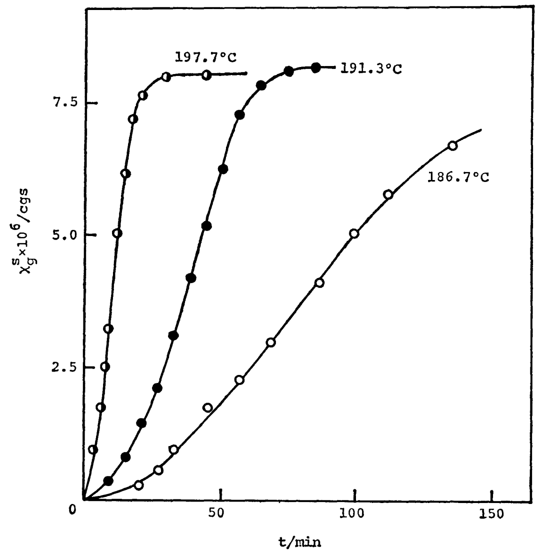

Fig. 5. ITM curves for diamagnetic Ni(N-Me-salam)$_2$; monomer-to-polymer transformation under isothermal conditions.

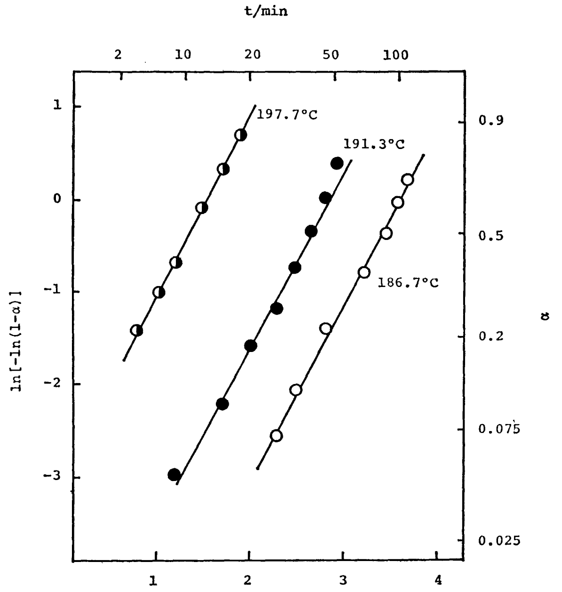

Fig. 6. Plots of ln[$-$ln(1$-\alpha$)] $vs.$ ln(t) for monomer-to-polymer transformation of Ni(N-Me-salam)$_2$.

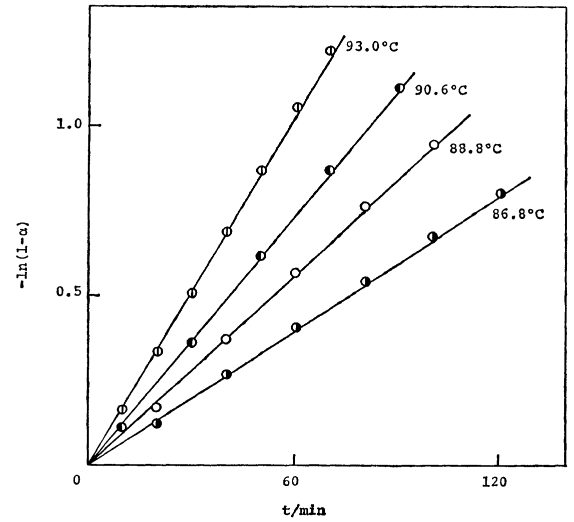

Fig. 7. First order rate plots for pyridine-liberating reaction of Ni(N-Ph-salam)$_2$py$_2$.

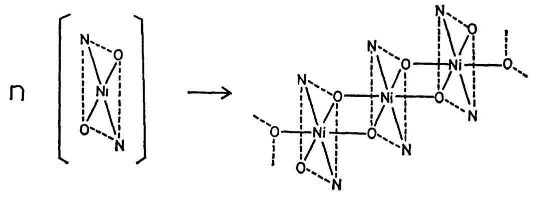

Fig. 8. Skeletal representation of monomer-to-polymer transformation.

in Fig. 6, the transformation isotherms thus obtained are well fitted to the Avrami-Erofeev equation:[18]

$$-\ln[-\ln(1-\alpha)] = (kt)^n. \quad [n=1.94\text{—}2.02] \qquad (5)$$

The kinetic parameters, E_a and A, were calculated to be 303 kJ/mol and 1×10^{33}, respectively.

For the purpose of comparison, the thermal dissociation reaction of the axial pyridine molecules of Ni(N-Ph-salam)$_2$py$_2$ has been subjected to kinetic analysis. The DSC curve of the adduct shown in Fig. 1-d exhibits two endothermic peaks at 140 and 280 °C; the former peak is accompanied by 26.0% weight-loss in the range 100—150 °C, which corresponds to the elimination of 2 mol of pyridine per mol of the adduct, while the latter one is accompanied by no weight-loss, and corresponds to the melting of the Form I isomer of Ni(N-Ph-salam)$_2$. The X-ray diffraction pattern of the sample obtained after heating at $ca.$ 150 °C was identical to that of an authentic Form I isomer. The pyridine-liberating reaction of the adduct could easily be followed by the isothermal weight-loss measurements. The liberation isotherms obtained at 86.8, 88.8, 90.6, and 93.0 °C fit well to the first order equation, as shown in Fig. 7. The kinetic parameters, E_a and A, were calculated to be 167 kJ/mol and 1×10^{22}, respectively.

Discussion

The polymerization reaction of Ni(N-Me-salam)$_2$ including the alteration of the spin-state of central Ni(II), singlet(monomer)-to-triplet(polymer), has been considered to progress through the further coordination of the phenolato oxygen atoms in the complex molecule to a Ni(II) ion of adjacent molecules at the apical position, forming octahedral coordination geometry around the Ni(II) ion, as drawn above.[8] The polymerization kinetics is found to be depicted by the Avrami-Erofeev equation with n=2, suggesting that the reaction rate is determined either by two dimensional growth of nuclei[19] or by random nucleation and one dimensional growth of nuclei.[20] By taking into account the fact that the proposed polymeric structure includes a one-dimensionally extended monomer, the latter model seems to be preferable for the present polymerization. On the other hand, the monomerization reaction of Ni(N-Ph-salam)$_2$ includes the spin-state alteration of Ni(II), triplet(polymer)-to-singlet(monomer); the monomerization kinetics fits the first order equation. The thermal pyridine liberating reaction of Ni(N-Ph-salam)$_2$py$_2$, which occurred with the accompanying triplet-to-singlet alteration of Ni(II) and the formation of monomeric Ni(N-Ph-salam)$_2$, is also depicted by the first order equation.

As shown in Table 2, the larger E_a and A values for the polymerization of Ni(N-Me-salam)$_2$ than those for the monomerization of Ni(N-Ph-salam)$_2$ could be understood by speculating that the progress of the polymerization requires more extensive movement of the molecules than that of the monomerization does.

We can compare the polymer complex and the pyridine adduct of Ni(N-Ph-salam)$_2$, both having octahedral and triplet Ni(II); the larger E_a value for the pyridine-liberating reaction than for the monomerization reaction seems to reflect a weaker association interaction than the adduct-formation interaction.

References

1) R. H. Holm and M. J. O'Connor, *Prog. Inorg. Chem.*, **14**, 241 (1971).

2) A. Takeuchi and S. Yamada, *Bull. Chem. Soc. Jpn.*, **44**, 1170 (1971).

3) A. Takeuchi and S. Yamada, *Inorg. Chim. Acta*, **8**, 225 (1974).

4) S. Yamada, K. Iwasaki, and A. Takeuchi, *Inorg. Chim. Acta*, **2**, 395 (1968).

5) R. H. Holm, *J. Am. Chem. Soc.*, **83**, 4683 (1961).

6) H. C. Clark and R. J. O'Brien, *Can. J. Chem.*, **39**, 1030 (1961).

7) L. Sacconi, P. Paoletti, and R. Cini, *J. Am. Chem. Soc.*, **80**, 3583 (1958).

8) C. M. Harris, S. L. Lenzer, and R. L. Martin, *Aust. J. Chem.*, **11**, 331 (1958).

9) N. Arai, M. Sorai, and S. Seki, *Bull. Chem. Soc. Jpn.*, **45**, 2398 (1972).

10) F. Basolo and W. R. Matoush, *J. Am. Chem. Soc.*, **75**, 5663 (1953).

11) W. Klem and K. H. Raddatz, *Z. Anorg. Allg. Chem.*, **250**, 207 (1942).

12) K. Miyokawa and I. Masuda, *J. Inorg. Nucl. Chem.*, **43**, 1495 (1981).

13) K. Shibata, "Methods of Biochemical Analysis," ed by D. Glick, Interscience, New York (1962), Vol. 4, p. 217.

14) W. W. Wendlandt, "Thermal Methods of Analysis," 2nd ed, John Wiley & Sons, New York (1974), p. 459.

15) K. Miyokawa and I. Masuda, *Fukuoka Univ. Science Reports*, **10**, 83 (1980).

16) A. B. P. Lever, "Inorganic Electronic Spectroscopy," Elsevier, Amsterdam (1968), p. 333.

17) "American Institute of Physics Handbook," 2nd ed, ed by D. E. Gray, McGraw-Hill, New York (1963), pp. 5—221.

18) M. Avrami, *J. Chem. Phys.*, **7**, 1103 (1939); **8**, 212 (1940); **9**, 177 (1941); B. V. Erofeev, *Dokl. Akad. Nauk SSSR*, **52**, 511 (1946).

19) O. Yamaguchi, M. Kamata, and K. Shimizu, *Bull. Chem. Soc. Jpn.*, **53**, 1973 (1980).

20) "Chemistry of Solid States," ed by W. E. Garner, Butterworth, London (1955), p. 184.